

$$\{F\} = \{N_x \ N_y \ N_{xy} \ M_x \ M_y \ M_{xy} \ Q_x \ Q_y\}^T$$

$$= \int_{-h/2}^{+h/2} \{\sigma_x, \sigma_y, \tau_{xy}, \sigma_{xz}, \sigma_{yz}, \tau_{xz}, \tau_{yz}\}^T dz \text{-----}$$

-----(3)

The stiffness coefficients are defined as:

$$A_{ij} = \sum_{k=1}^{np} (Q_{ij})_k (z_k - z_{k-1})$$

$$B_{ij} = \frac{1}{2} \sum_{k=1}^{np} (Q_{ij})_k (z_k^2 - z_{k-1}^2)$$

$$D_{ij} = \frac{1}{3} \sum_{k=1}^{np} (Q_{ij})_k (z_k^3 - z_{k-1}^3) \quad i, j = 1, 2, 6$$

$$S_{ij} = \sum_{k=1}^{np} F_i F_j (G_{ij})_k (z_k - z_{k-1}) \quad i, j = 1, 2 \text{-----}$$

----- (4)

Where Q_{ij} are elements of the off-axis elastic constant matrix, which are derived by appropriate transformation of on-axis matrix which contains the basic elasticity terms of the laminae as reported earlier [10]:

$$[Q_{ij}]_{off} = [T]^T [Q_{ij}]_{on} [T] \text{-----}$$

----- (5)

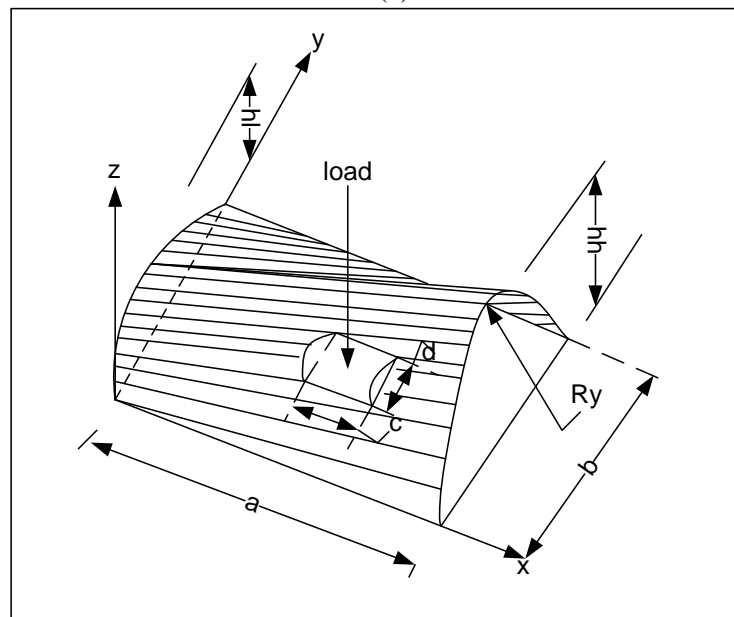


Fig.1 Conoidal shell

The strain-displacement relations on the basis of improved first order approximation theory for thin shell are established as:

$$\{\epsilon_x, \epsilon_y, \gamma_{xy}, \gamma_{xz}, \gamma_{yz}\}^T = \{\epsilon_x^0, \epsilon_y^0, \gamma_{xy}^0, \gamma_{xz}^0, \gamma_{yz}^0\}^T$$

$$+ z \{\kappa_x, \kappa_y, \kappa_{xy}, \kappa_{xz}, \kappa_{yz}\}^T \text{-----}$$

----- (6)

Where the first vector is the mid-surface strain for conoidal shell and the second vector is the change of curvature due to loadings. These are given, respectively, by:

$$\begin{Bmatrix} 0 \\ \varepsilon_x \\ 0 \\ \varepsilon_y \\ 0 \\ \gamma_{xy} \\ 0 \\ \gamma_{xz} \\ 0 \\ \gamma_{yz} \end{Bmatrix} = \begin{Bmatrix} \partial u / \partial x \\ \partial v / \partial y - w / R_y \\ \partial u / \partial y + \partial v / \partial x - 2w / R_{xy} \\ \alpha + \partial w / \partial x \\ \beta + \partial w / \partial y \end{Bmatrix},$$

$$\begin{Bmatrix} \kappa_x \\ \kappa_y \\ \kappa_{xy} \\ \kappa_{xz} \\ \kappa_{yz} \end{Bmatrix} = \begin{Bmatrix} \partial \alpha / \partial x \\ \partial \beta / \partial y \\ \partial \alpha / \partial y + \partial \beta / \partial x \\ 0 \\ 0 \end{Bmatrix},$$

----- (7)

The radius of curvature may be evaluated by differentiating the surface equation of shell in the form $z=f(x, y)$ and for shallow shells, which are taken up for the present study, the same may be expressed as:

$$\frac{1}{R_{xy}} = \frac{\partial^2 z}{\partial x \partial y} \quad \text{And} \quad \frac{1}{R_y} = \frac{\partial^2 z}{\partial y^2}$$

B. Finite Element Formulation [10]

1) *Finite Element Formulation for the Shell Element:* An eight noded isoparametric curved quadratic shell element with five degrees of freedom u, v, w, α, β at each node (displacements along x, y and z axes and rotations about y and x axes) is used in the present shell analysis as appears in Reference [10].

2) *Element Stiffness Matrix*

The strain-displacement relations when cast in the terms of finite element formulation assume the following form:

$$\{\varepsilon\} = [B] \{d_e\} \tag{8}$$

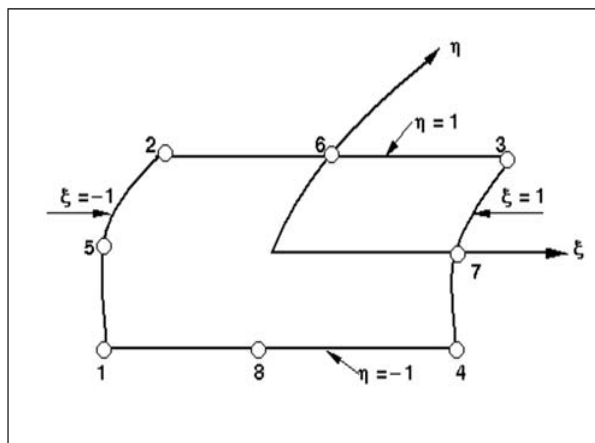


Fig. 2 Eight noded curved quadratic isoparametric element

Where,

$$\{d_e\} = [u_1 \ v_1 \ w_1 \ \alpha_1 \ \beta_1 \ \dots \ u_8 \ v_8 \ w_8 \ \alpha_8 \ \beta_8]^T,$$

$$[B] = \sum_{i=1}^8 \begin{bmatrix} N_{ix} & 0 & 0 & 0 & 0 \\ 0 & N_{iy} & -N_i/R_y & 0 & 0 \\ N_{iy} & N_{ix} & -2N_i/R_{xy} & 0 & 0 \\ 0 & 0 & 0 & N_{ix} & 0 \\ 0 & 0 & 0 & 0 & N_{iy} \\ 0 & 0 & 0 & N_{iy} & N_{ix} \\ 0 & 0 & N_{ix} & N_i & 0 \\ 0 & 0 & N_{iy} & 0 & N_i \end{bmatrix} \text{----- (9)}$$

The element stiffness matrix is:

$$[K_{she}] = \iint [B]^T [D] [B] dx dy \text{----- (10)}$$

The two-dimensional integration is carried out by reduced integration using 2x2 Gauss quadrature, because the shape functions are derived from cubic interpolation polynomial

3) *Element Load Vector:* The consistent load vector {P_e} is given by:

$$\{P_e\} = \iint_A [N]^T \{q\} dx dy \text{----- (11)}$$

Where, {q} = { 0 0 q 0 0 } for transversely loaded shell and scalar q is the intensity of uniformly distributed transverse load.

The area integral is evaluated by Gauss quadrature like the stiffness matrix.

4) *Solution Procedure:* The element stiffness matrix and the element load vectors are assembled to get the global matrices, on which the boundary conditions are imposed by deleting the rows and columns of the above matrices corresponding to zero boundary values. Thus the basic problem of statics takes the form:

$$[K]\{d\} = \{P\} \text{----- (12)}$$

Where [K] is the overall stiffness matrix and {d} and {P} are generalized displacement and load vectors, respectively. The above equation is solved by the Gauss elimination technique, and from the global displacement vector {d} thus obtained, the element displacement vectors {d_e} are calculated. Using {d_e} in Equation (8) the strains are evaluated at the Gauss points, which when put in equation (1) the generalized force and moment resultants are obtained at those points. These values are extrapolated to obtain the nodal values of the forces and moments

III. NUMERICAL EXAMPLES

The correctness of the present approach is confirmed by solving two benchmark problems. The first one concerns deflection of isotropic conoidal shell under uniformly distributed loading, which was solved earlier by Hadid and Das and Chakravorty (10). The results of the first benchmark problem are presented graphically in figure, where deflections at different sections are plotted. The second benchmark problem, regarding bending of laminated composite conoidal shells was solved earlier by Das & Chakravorty (10). Table I contains values of maximum non-dimensional downward deflection of 0⁰/90⁰ and 0⁰/90⁰/0⁰ laminates obtained by Das & Chakravorty (10) and by the present authors. Various other problems which are authors' own are solved to study the bending behaviour of laminated composite conoidal shells under uniformly distributed pressure with clamped boundary conditions and anti-symmetric and symmetric stacking sequences by varying aspect ratio and degree of truncation.

IV. NUMERICAL RESULTS AND DISCUSSION

The results of the comparative problems and then of the additional examples are discussed in the following sections.

A. Comparative Problems

The results of first benchmark problem are presented graphically in fig. where the deflections at different sections are plotted. The graph obtained by Hadid and Das and Chakravorty (10) and that obtained by the present method showed very close agreement. This confirms the correct incorporation of conoidal shell curvature in the present approach.

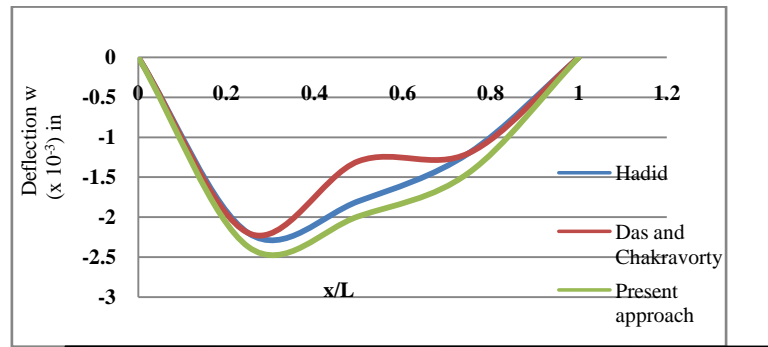


Fig.3 Deflection of isotropic conoid under uniformly distributed load along $y=0.5$.

$a=95\text{in}$, $b=95\text{in}$, $h=18\text{in}$, $h_l=9\text{in}$, $h=0.5\text{in}$, $E=5620000\text{psi}$, $\nu=0.15$ and $q=60\text{psf}$

$a/b=1$, $a/h=1$, $h_l/h=0.25$, $E_{11}=25E_{22}$, $G_{12}=G_{13}=0.5 E_{22}$, $G_{23}=0.2 E_{22}$, $\nu=0.25$

The results of second problems are shown in the table I which showed the close agreement of present and benchmark results. Hence the correctness of the laminated shell formulation is established.

Table I

Values of maximum non-dimensional downward deflection ($\bar{w} \times 10^4$) for different laminations and clamped edge boundary condition.

Lamination	Das & Chakravorty (2007)	Present Approach
$0^0/90^0$	-0.319	-0.344
$0^0/90^0/0^0$	-0.298	-0.309

B. Additional Examples

Tables II, III and IV and Figs. 4-9 present the results of the additional examples of maximum transverse non-dimensional downward deflections of laminated having different anti-symmetric and symmetric stacking sequences by varying aspect ratio and degree of truncation for clamped boundary conditions, these examples are taken up for discussion in the following sections.

1. *Behaviour of Clamped Shells under Uniformly Distributed Pressure:* Maximum non-dimensional downward deflection for clamped boundary conditions under uniformly distributed pressure is shown in Table II, III and IV. From the observation of results it is seen that the deflection decreases with increase in degree of truncation and aspect ratio. It shows that the bending stiffness of the clamped conoidal shell increases with increase in aspect ratio. The results also lead to infer that a truncated conoidal shell is stiffer than a full conoid from bending point of view and this stiffness increases further with the increase of h_l/h Ratio.

2. *Antisymmetric vs. Symmetric lamination:* The symmetric laminates are found to be stronger than the anti-symmetric laminates with respect to bending stiffness for different aspect ratio and degree of truncation shown in Fig (4-9). The superior performance of $(90^0/0^0/0^0/90^0)$ lamination scheme having four symmetric layers is observed from the lowest value of \bar{w} out of all the values furnished in Table II& III. But for aspect ratio =2 it shows lower deflection only for $h_l/h=0$ and $h_l/h=0.05$ as compared to other lamination schemes. The non-dimensional downward deflection of the two anti-symmetric four layered lamination scheme $(0^0/90^0/0^0/90^0)$ and $(90^0/0^0/90^0/0^0)$ are found to be same for different aspect ratio and degree of truncation. Similarly, the two anti-symmetric two layers lamination scheme $(0^0/90^0)$ and $(90^0/0^0)$ are also showing approximately same values of w for all the values of h_l/h and a/b except for shell with $a/b=2$ and $h_l/h=0, 0.05$.

Effect of Increasing the Number of Layers: In order to study the effect of increase of no. of layers on maximum non-dimensional downward deflection, comparative study is done for both anti-symmetric and symmetric laminations in this paper. When we compare two layered $(0^0/90^0)$ and $(90^0/0^0)$ and four layered $(0^0/90^0)_2$ and $(90^0/0^0)_2$ anti-symmetric cross plies, from composite conoidal shell roofs under uniformly distributed pressure with cross ply laminates

3. Fig. (4-9) it is seen that increase in number of plies has positive effect in decreasing the deflection values for all a/b ratios and h_l/h ratios. Comparison among three layered symmetric $(0^0/90^0/0^0)$ and $(90^0/0^0/90^0)$ and four layered symmetric $(0^0/90^0)_s$ and $(90^0/0^0)_s$ cross ply shells is also done and it is noticed that deflection decrease with

increase in number of layers and h_l/h_h except for $(0^0/90^0)_s$ lamination for a/b ratio=0.5, 1 shown in Fig 5&7 . But for $a/b=2$ deflection decrease with increase in number of layers only in case $h_l/h_h=0$ and $h_l/h_h=0.05$ $(0^0/90^0)_s$ being exception in all cases. It is also observed that $a/b=2$, $h_l/h_h= (0.1-0.3)$ $(0^0/90^0/0^0)$ showed lower deflection and $(90^0/0^0/90^0)$ showed higher deflection with increase h_l/h_h ratio from 0.05 to 0.3 compared to other lamination schemes.

This observation leads to an important conclusion that if anti-symmetric laminations are considered then greater number of plies should be preferred but for symmetric ones one cannot conclude confidently whether the number of plies shall be maintained less or more in number for better performance, case specific study has to be carried out.

Table II

Maximum non-dimensional downward deflections ($w \times 10^4$) clamped laminated conoidal shells with aspect ratio = 0.5 under uniformly distributed pressure with different laminations and degree of truncation.

Lamination (Deg)	Degree of Truncation (h_l/h_h)						
	0.3	0.25	0.2	0.15	0.1	0.05	0
$0^0/90^0$	-2.874 (0.38,0.5)	-3.277 (0.42,0.5)	-3.74 (0.36,0.5)	-4.271 (0.39,0.5)	-4.879 (0.39,0.5)	-5.572 (0.42,0.5)	-6.357 (0.42,0.5)
$90^0/0^0$	-2.923 (0.39,0.5)	-3.335 (0.39,0.5)	-3.809 (0.39,0.5)	-4.353 (0.39,0.5)	-4.977 (0.39,0.5)	-5.688 (0.36,0.5)	-6.493 (0.42,0.5)
$0^0/90^0/0^0$	-2.821 (0.31,0.5)	-3.218 (0.33,0.5)	-3.686 (0.35,0.5)	-4.238 (0.36,0.5)	-4.89 (0.35,0.5)	-5.658 (0.34,0.5)	-6.558 (0.36,0.5)
$90^0/0^0/90^0$	-2.622 (0.44,0.5)	-2.87 (0.47,0.5)	-3.142 (0.47,0.5)	-3.44 (0.47,0.5)	-3.764 (0.47,0.5)	-4.115 (0.47,0.5)	-4.492 (0.47,0.5)
$0^0/90^0/0^0/90^0$	-2.432 (0.42,0.5)	-2.703 (0.42,0.5)	-3.008 (0.39,0.5)	-3.35 (0.39,0.5)	-3.731 (0.42,0.5)	-4.157 (0.36,0.5)	-4.628 (0.42,0.5)
$90^0/0^0/90^0/0^0$	-2.448 (0.42,0.5)	-2.723 (0.42,0.5)	-3.031 (0.47,0.5)	-3.376 (0.47,0.5)	-3.762 (0.42,0.5)	-4.192 (0.44,0.5)	-4.669 (0.47,0.5)
$0^0/90^0/90^0/0^0$	-3.051 (0.39,0.5)	-3.423 (0.39,0.5)	-3.85 (0.36,0.5)	-4.339 (0.39,0.5)	-4.897 (0.36,0.5)	-5.532 (0.39,0.5)	-6.248 (0.36,0.5)
$90^0/0^0/0^0/90^0$	-2.03 (0.42,0.5)	-2.243 (0.42,0.5)	-2.479 (0.42,0.5)	-2.741 (0.36,0.5)	-3.031 (0.44,0.5)	-3.349 (0.36,0.5)	-3.696 (0.39,0.5)

Note: $a/h = 100$, $a/h_h = 5$, $E_{11} = 25E_{22}$, $G_{12} = G_{13} = 0.5 E_{22}$, $G_{23} = 0.2 E_{22}$, $\nu = 0.25$

Values in the parentheses indicate the location (x^- , y^-) of maximum downward deflection in each case.

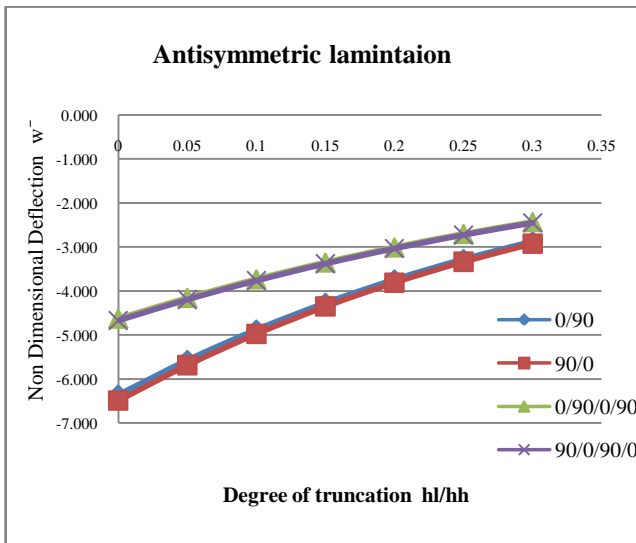


Fig. 4 Graphical variation of w^- with different degree of truncation and aspect ratio = 0.5 for clamped antisymmetric laminated shell.

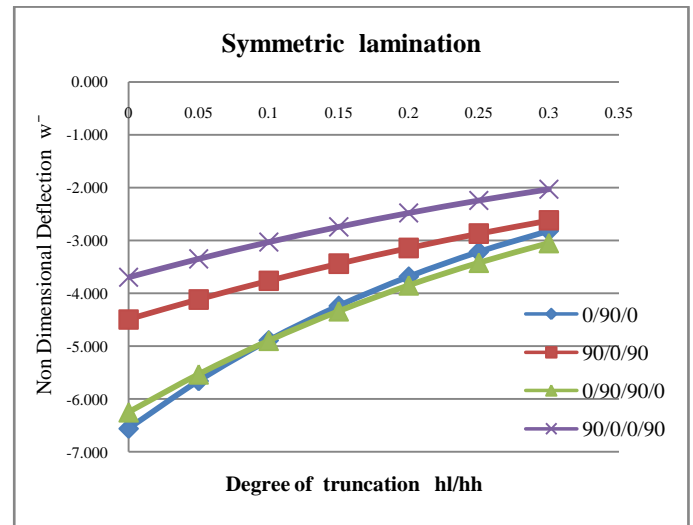


Fig.5 Graphical variation of w^- with different degree of truncation and aspect ratio=0.5 for clamped symmetric laminated shell.

Table III

Maximum non-dimensional downward deflections $w^- \times 10^4$ clamped laminated conoidal shells with aspect ratio = 1 under uniformly distributed pressure with different laminations and degree of truncation.

Lamination (deg)	Degree of truncation (hl/hh)						
	0.3	0.25	0.2	0.15	0.1	0.05	0
0 ⁰ /90 ⁰	-0.304 (0.26,0.5)	-0.358 (0.26,0.5)	-0.425 (0.26,0.5)	-0.51 (0.26,0.5)	-0.619 (0.26,0.5)	-0.759 (0.26,0.5)	-0.94 (0.26,0.5)
90 ⁰ /0 ⁰	-0.309 (0.26,0.5)	-0.365 (0.26,0.5)	-0.434 (0.25,0.5)	-0.522 (0.25,0.5)	-0.622 (0.25,0.5)	-0.779 (0.25,0.5)	-0.966 (0.26,0.5)
0 ⁰ /90 ⁰ /0 ⁰	-0.259 (0.23,0.5)	-0.306 (0.21,0.5)	-0.367 (0.25,0.5)	-0.447 (0.24,0.5)	-0.553 (0.25,0.5)	-0.695 (0.25,0.5)	-0.888 (0.21,0.5)
90 ⁰ /0 ⁰ /90 ⁰	-0.323 (0.36,0.5)	-0.371 (0.39,0.5)	-0.427 (0.36,0.5)	-0.494 (0.34,0.5)	-0.574 (0.34,0.5)	-0.669 (0.34,0.5)	-0.782 (0.34,0.5)
0 ⁰ /90 ⁰ /0 ⁰ /90 ⁰	-0.271 (0.29,0.5)	-0.314 (0.28,0.5)	-0.366 (0.29,0.5)	-0.429 (0.26,0.5)	-0.508 (0.29,0.5)	-0.606 (0.28,0.5)	-0.727 (0.27,0.5)
90 ⁰ /0 ⁰ /90 ⁰ /0 ⁰	-0.274 (0.29,0.5)	-0.317 (0.28,0.5)	-0.37 (0.26,0.5)	-0.435 (0.29,0.5)	-0.516 (0.26,0.5)	-0.615 (0.31,0.5)	-0.739 (0.27,0.5)
0 ⁰ /90 ⁰ /90 ⁰ /0 ⁰	-0.311 (0.26,0.5)	-0.363 (0.21,0.5)	-0.429 (0.31,0.5)	-0.511 (0.26,0.5)	-0.617 (0.21,0.5)	-0.751 (0.26,0.5)	-0.924 (0.25,0.5)
90 ⁰ /0 ⁰ /0 ⁰ /90 ⁰	-0.241 (0.31,0.5)	-0.277 (0.34,0.5)	-0.32 (0.36,0.5)	-0.372 (0.31,0.5)	-0.435 (0.31,0.5)	-0.511 (0.34,0.5)	-0.603 (0.32,0.5)

Note: $a/h = 100$, $a/hh = 5$, $E_{11} = 25E_{22}$, $G_{12} = G_{13} = 0.5 E_{22}$, $G_{23} = 0.2 E_{22}$, $\nu = 0.25$

Values in the parentheses indicate the location (x^- , y^-) of maximum downward deflection in each case.

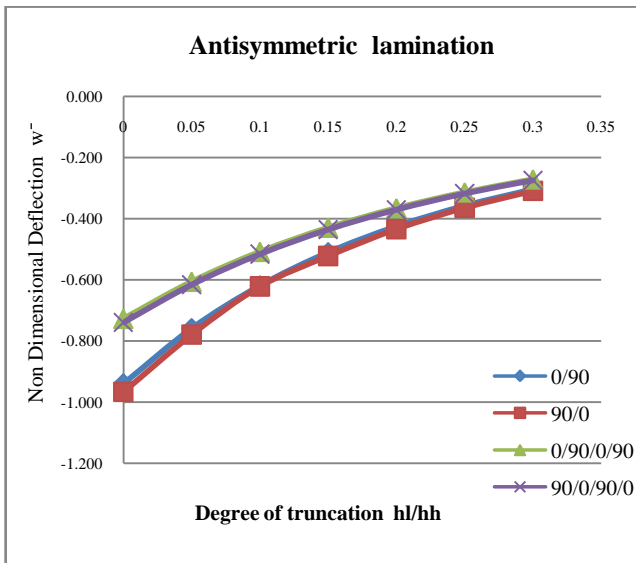


Fig. 6 Graphical variation of w^- with different degree of truncation and aspect ratio = 1 for clamped antisymmetric laminated shell.

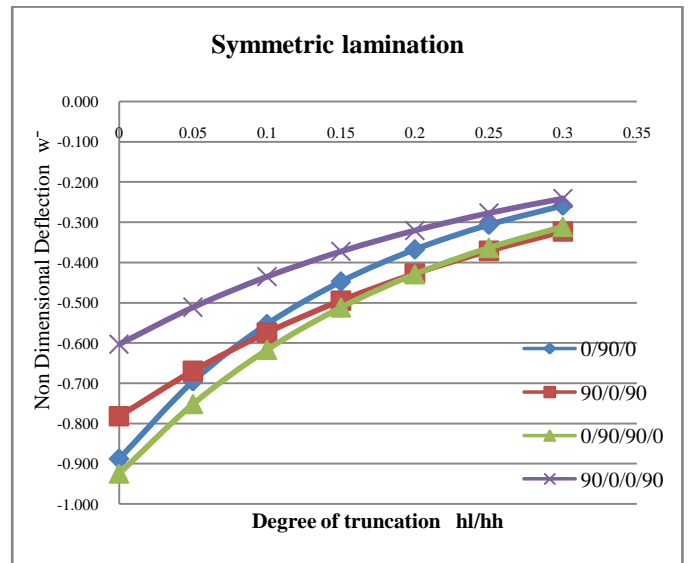


Fig.7 Graphical variation of w^- with different degree of truncation and aspect ratio = 1 for clamped symmetric laminated shell.

Table IV

Maximum non-dimensional downward deflections $w \times 10^4$ clamped laminated conoidal shells with aspect ratio = 2 under uniformly distributed pressure with different laminations and degree of truncation.

Lamination (deg)	Degree of truncation (hl/hh)						
	0.3	0.25	0.2	0.15	0.1	0.05	0
0°/90°	-0.03 (0.18,0.5)	-0.036 (0.18,0.5)	-0.043 (0.19,0.5)	-0.056 (0.16,0.5)	-0.072 (0.15,0.5)	-0.097 (0.14,0.5)	-0.137 (0.17,0.5)
90°/0°	-0.031 (0.18,0.5)	-0.037 (0.21,0.5)	-0.045 (0.17,0.5)	-0.058 (0.16,0.5)	-0.075 (0.18,0.5)	-0.102 (0.18,0.5)	-0.145 (0.18,0.5)
0°/90°/0°	-0.022 (0.15,0.5)	-0.026 (0.16,0.5)	-0.032 (0.16,0.5)	-0.043 (0.14,0.5)	-0.057 (0.15,0.5)	-0.079 (0.15,0.5)	-0.115 (0.18,0.5)
90°/0°/90°	-0.039 (0.21,0.5)	-0.045 (0.21,0.5)	-0.053 (0.21,0.5)	-0.062 (0.21,0.5)	-0.077 (0.21,0.5)	-0.097 (0.19,0.5)	-0.125 (0.21,0.5)
0°/90°/0°/90°	-0.028 (0.21,0.5)	-0.033 (0.21,0.5)	-0.039 (0.18,0.5)	-0.05 (0.18,0.5)	-0.064 (0.17,0.5)	-0.084 (0.18,0.5)	-0.115 (0.19,0.5)
90°/0°/90°/0°	-0.028 (0.19,0.5)	-0.034 (0.19,0.5)	-0.04 (0.21,0.5)	-0.052 (0.15,0.5)	-0.066 (0.18,0.5)	-0.087 (0.17,0.5)	-0.119 (0.18,0.5)
0°/90°/90°/0°	-0.029 (0.21,0.5)	-0.034 (0.18,0.5)	-0.041 (0.17,0.5)	-0.054 (0.16,0.5)	-0.07 (0.18,0.5)	-0.093 (0.17,0.5)	-0.13 (0.18,0.5)
90°/0°/0°/90°	-0.028 (0.21,0.5)	-0.032 (0.21,0.5)	-0.039 (0.21,0.5)	-0.047 (0.16,0.5)	-0.059 (0.17,0.5)	-0.076 (0.17,0.5)	-0.102 (0.18,0.5)

Note: $a/h = 100$, $a/hh = 5$, $E_{11} = 25E_{22}$, $G_{12} = G_{13} = 0.5 E_{22}$, $G_{23} = 0.2 E_{22}$, $\nu = 0.25$

Values in the parentheses indicate the location (x^-, y^-) of maximum downward deflection in each case.

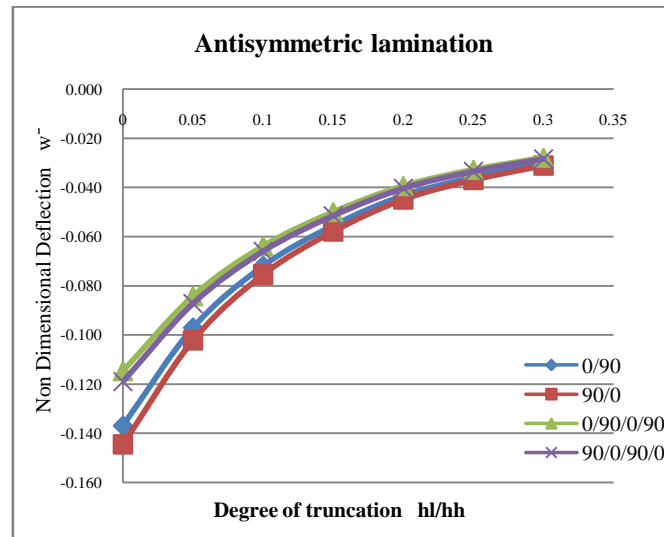


Fig. 8 Graphical variation of w^- with different degree of truncation and aspect ratio =2 for clamped anti-symmetric laminated shell.

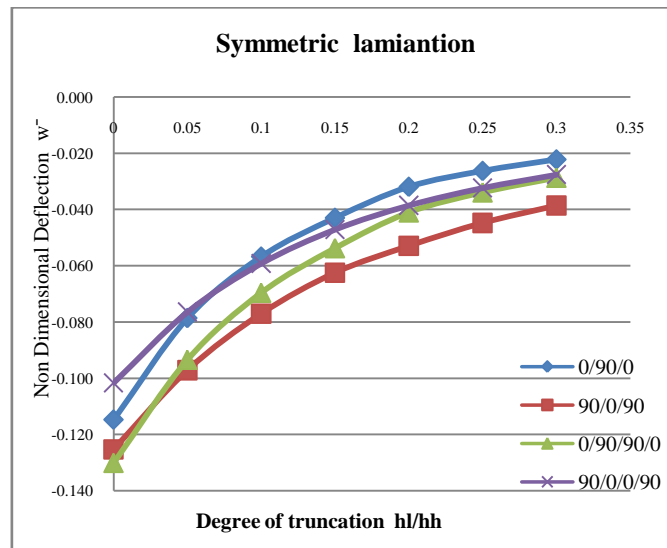


Fig.9 Graphical variation of w^- with different degree of truncation and aspect ratio=2 for clamped symmetric laminated shell.

V. CONCLUSION

The following are the conclusions drawn from the present study.

1. The finite element formulation presented in this project can be successfully applied to analyse bending problems of laminated composite conoidal shells which is clear from the results of the benchmark problems presented in the project.
2. Bending stiffness of laminated composite conoidal shells is found to increase with increase in aspect ratio.
3. The results also lead to infer that a truncated conoidal shell is stiffer than a full conoidal shell from bending point of view and this stiffness increases further with increase of hl/hh ratio.
4. For a clamped laminated composite conoidal shell, symmetric laminates are found to be stronger than the anti-symmetric laminates with respect to bending stiffness for different aspect ratio and degree of truncation. For this boundary condition an increase in number of laminae is good for anti-symmetric laminates, but for symmetric laminates such a conclusion does not hold.

NOTATIONS

a, b length and width of shell in plan along beam and arch directions respectively

c, d	length and width of delamination area in plan along beam and arch directions respectively
E_{11}, E_{22}	elastic moduli
{F}	force and moment resultant
G_{12}, G_{13}, G_{23}	shear moduli of a lamina with respect to 1, 2 and 3 axes of fiber
h	shell thickness
hh	greater height of conoid
hl	smaller height of conoid
{ κ }	curvature changes due to loading
$\kappa_x, \kappa_y, \kappa_{xy}$	curvatures of shell
{M}	moment vectors
M_x, M_y	moment resultants
M_{xy}	torsion resultant
{N}	force vectors
N_x, N_y	Inp lane force resultants
N_{xy}	In plane shear resultant
q	Magnitude of distributed load
{Q}	transverse shear force vectors
Q_x, Q_y	transverse shear resultants
[Q_{ij}]	elastic constant matrix
R_y	radius of shell surface along arch (y)direction
R_{xy}	radii of cross curvature of shell
[S]	stiffness matrix in transverse shear
u, v, w	translational degrees of freedom at each node of shell element
α, β	rotational degrees of freedom at each node of shell element
{ ϵ }	inplane strain vectors
{ γ }	transverse shear strain vectors
{ ν_{12} }	Poisson's ratio
ξ, η	local natural co-ordinates of an element
w	non-dimensional deflection, where $\bar{w} = (wh^3 E22 / Pa^4) \times 10^4$
ρ	density of material
w	vertical deflection
{ d_e }	element displacement
N_1-N_8	shape functions
x, y, z	local co-ordinate axes
X, Y, Z	global co-ordinate axes
α, β	rotational degrees of freedom
ϵ_x, ϵ_y	inplane strain components

REFERENCES

- [1] Choi C. K., "A conoidal shell analysis by modified isoparametric element", *Journal of Computers & Structures*, vol.18 (5), pp 921–924, 1984.
- [2] Ghosh B., and Bandopadhyay J. N., Bending analysis of conoidal shells using curved quadratic isoparametric element, *Journal of Computers & Structures*, vol.33, pp 717–728, 1989.
- [3] Ghosh B and Bandopadhyay J. N., "Approximate bending analysis of conoidal shells using the Galerkin method", *Journal of Computers & Structures*, vol. 36(5), pp 801–805, 1990.
- [4] Dey A., Bandyopadhyay J. N., and Sinha P. K., "Finite element analysis of laminated composite conoidal shell structures", *Journal of Computers & Structures*, vol. 43(3), pp 469–476, 1992.
- [5] Das A. K., and Bandopadhyay J. N., "Theoretical and experimental studies on conoidal shells", *Journal of Computers & Structures*, vol.49 (3), pp 531–536, 1993.
- [6] Ghosh B., and Bandopadhyay J. N., "Bending analysis of conoidal shells with cut-outs, *Journal of Computers & Structures*", vol. 53(1), pp 9–18, 1994.
- [7] Chakravorty D., Bandyopadhyay J. N., and Sinha P. K., Finite element free vibration analysis of conoidal shells, *Journal of Computers & Structures*, vol. 56(6), pp 975–978, 1995.
- [8] Nayak A. N., and Bandopadhyay J. N., "Free vibration analysis and design aids of stiffened conoidal shells, *Journal of Engineering Mechanics*", vol.128, pp 419-427, 2002.
- [9] Nayak A. N., and Bandopadhyay J. N., "Dynamic response analysis of stiffened conoidal shells, *Journal of Sound Vibration*, vol. 291(3–5), pp 1288–1297, 2006.
- [10] Das H. S., and Chakravorty D., "Design aids and selection guidelines for composite conoidal shell roofs – a finite element application", *Journal of Reinforced Plastics and Composite*, vol. 26(17), pp 1793–1819, 2007.
- [11] Pradyumna S., and Bandopadhyay J. N., "Static and free vibration analyses of laminated shells using a higher order theory", *Journal of Reinforced Plastics and Composite*, vol. 27(2), pp 167–186, 2008.
- [12] Das H. S., and Chakravorty D., "Natural frequencies and mode shapes of composite conoids with complicated boundary conditions", *Journal of Reinforced Plastics and Composite*, vol. 27(13), pp 1397–1415, 2008.
- [13] Das H. S., and Chakravorty D., "A finite element application in the analysis and design of point-supported composite conoidal shell roof: suggesting selection guidelines", *Journal of Reinforced Plastics and Composite*, vol. 45(3), pp 165–177, 2010.
- [14] S. Kumari and D. Chakravorty, "On the bending characteristics of damaged composite conoidal shells- a finite element approach", *Journal of Reinforced Plastics and Composite*, vol. 29(21), pp 3287–3296, 2010.
- [15] Bakshi K., Das S. H., and Chakravorty D., "Forced motions of composite conoidal shell roofs with complicated boundary conditions", *Journal of advanced materials research*, vol. 123 –125, pp 89 – 92, 2010.
- [16] S. Kumari and D. Chakravorty, "Study of static characteristics of delaminated composite conoidal shell subjected to point load", *Journal of advanced materials research*, vol. 123 – 125, pp 455 – 458, 2010.
- [17] S. Kumari and D. Chakravorty, "Finite element bending behaviour of discretely delaminated composite conoidal shell roofs under concentrated load", *Journal of engineering mechanics, ASCE*, vol. 2 (4), pp 54–70, 2010.
- [18] S. Kumari and D. Chakravorty, "Bending of delaminated composite conoidal shells under uniformly distributed load", *Journal of engineering mechanics, ASCE*, vol. 137 (10), pp 660 – 668, 2011.
- [19] Das S. H., and Chakravorty D., "Bending analysis of stiffened composite conoidal shell roofs through finite element application", *Journal of composite materials*, vol. 45(5), pp 525-542, 2011.
- [20] Pradhan N., and Jena J., "Static characteristics of stiffened conoidal shell roofs under concentrated load", *IJAET*, vol. 4(2), pp 195-205, 2012.